RAA 2019 Vol. **19** No. **6**, 86(12pp) doi: 10.1088/1674–4527/19/6/86

http://www.raa-journal.org *http://iopscience.iop.org/raa*

Research in Astronomy and Astrophysics

Dish Verification Antenna China for the SKA: design, verification and status

Biao Du[1,2], Yang Wu[1,2,3], Yuan-Peng Zheng[1,2], Xiao-Ming Chai[2,3], Guo-Xi Liu[1], Hai-Dong Wang[1], Yi-Fan Zhang[1], Sheng-Hua Yu[2,3], Bin Liu[2,3], Ye-Zhao Yu[2,3], Hong-Wei Xi[2,3], Long Chen[1], Lei Yu[2,3], Dong-Liang Liu[2,3], Cheng-Jin Jin[2,3] and Bo Peng[2,3]

[1] The $54^{\rm th}$ Research Institute of CETC, Shijiazhuang 050081, China
[2] Joint Laboratory of Radio Astronomy Technology, Beijing 100101, China; *ywu@nao.cas.cn*
[3] National Astronomical Observatories, Chinese Academy of Sciences, Beijing 100101, China

Received 2019 January 14; accepted 2019 February 17

Abstract The Square Kilometre Array (SKA) will be the world's largest synthesis radio telescope, which is designed to answer major scientific questions such as those relating to the cosmic origin and fundamental forces in the universe. With the SKA entering into the phase of pre-construction, more than 100 institutes in about 20 countries including China have been involved in the associated key technology development. The Dish Verification Antenna China (DVA-C) is a concept prototype which has been built to meet the requirements of the SKA's scientific goals. It utilizes a unique skin-and-rib structure with single-piece panel reflectors. This paper presents details on the design and measured performances of DVA-C, as well as the preliminary observational results. Current applications of the DVA-C are also introduced.

Key words: Square Kilometre Array — radio telescope — dish — single-piece panel

1 INTRODUCTION

The Square Kilometre Array (SKA) (Dewdney et al. 2009) will be the world's largest radio telescope, providing unparalleled sensitivity and great opportunities for important discoveries and scientific breakthroughs. Given this great ambition for the 21st century, the SKA will confront tremendous challenges in radio astronomy. A worldwide consortium composed of universities and institutions from more than ten countries has been established, called the SKA organization (SKAO), which is headquartered in Manchester in the UK. After two decades of effort, several pathfinders and precursors, implementing different concepts, have been built and demonstrated (Hampson et al. 2012; van Ardenne et al. 2009; Hovey et al. 2014; Davidson et al. 2012; Yang et al. 2014; Akgiary et al. 2013; de Lera et al. 2012; Imbriale et al. 2011), and a hybrid concept consisting of a Low Frequency Aperture Array (LFAA), Dish Array (DA) and Middle Frequency Aperture Array (MFAA) will be adopted. As a co-founder and one of the 10 member countries of SKAO, China participated in several work packages in the SKA pre-construction phase, and an important contribution to the SKA project is the proposal of the Dish Verification Antenna China (DVA-C) (Peng et al. 2012).

The DVA-C concept was first proposed at the SKA concept design review (CoDR), held in Penticton, Canada in 2011, including an option of offset Gregorian antenna (DVAC-1) and another one of primary focus antenna (DVAC-2). After two years of intensive R&D efforts, the first option was selected and now DVA-C is an offset Gregorian antenna with a 15 m diameter aperture and feed-up structure. The DVA-C antenna adopts single-piece main/sub-reflectors, consisting of a 2 mm thick carbon fiber skin and several sandwich structure composite backing ribs, based on some existing engineering experience and advanced technology concepts. A turning-head altazimuth mount is employed to achieve a wide motion range at a reasonable cost.

Table 1 shows the specifications of the DVA-C in terms of design, according to the SKA stage 1 system baseline design (Dewdney et al. 2013).

In August 2014, the integration of DVA-C was completed (Fig. 1), and we advanced into the verification stage, together with another two SKA dish prototypes: DVA-1

Table 1 Specifications of DVA-C

Items	Specifications
Antenna type	Offset Gregorian, feed-up
Equivalent physical aperture diameter	15 m
Mount type	Altazimuth (AZ: full-motion, EL: screw)
Reflector structure	Carbon fiber single-piece reflectors
Frequency range	0.35–20 GHz
Aperture efficiency	350 MHz: $\sim$60%, 400 MHz: $\sim$65%, 0.6–8 GHz: $\sim$78%, 8–15 GHz: $\sim$70%, 15–20 GHz: $\sim$65%
Polarization	Dual linear
$1^{\rm st}$ sidelobe	≤ -21 dB
Polarization purity	–30 dB (Within HPBW)
Pointing accuracy	$\leq$ 10$''$ rms (Precision) $\leq$ 17$''$ rms (Standard) $\leq$ 180$''$ rms (Degradation)
Travel range	AZ: $-270° \sim 270°$, EL: $15° \sim 95°$
Slew rates (Max)	AZ: $3° \mathrm{s}^{-1}$, EL: $1° \mathrm{s}^{-1}$
Acceleration (Max)	AZ: $3° \mathrm{s}^{-2}$, EL: $0.5° \mathrm{s}^{-2}$
Ambient temperature	$-10°\mathrm{C} \sim 55°\mathrm{C}$
Wind velocity	Drive to stow: 70 km h^{-1} Survival: 160 km h^{-1} (at El$= 54°$)
Expected lifetime	$\geq$ 30 years

Fig. 1 Photograph of DVA-C.

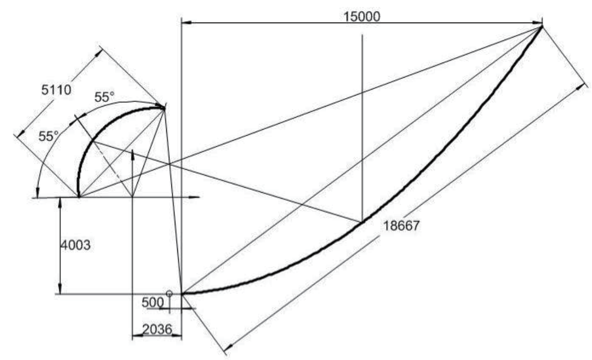

Fig. 2 Optical Design of the DVA-C.

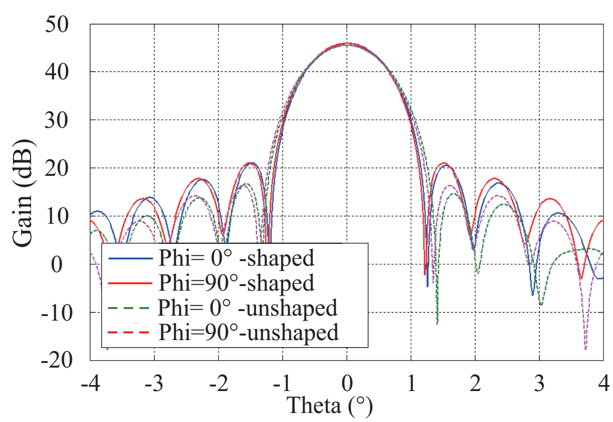

Fig. 3 Simulated DVA-C Radiation Pattern at 1.4 GHz.

in Canada (Hovey et al. 2014) and MeerKAT-1 in South Africa (Davidson et al. 2012).

This paper presents details on the DVA-C design, including the dish optics, elevation assembly, mount and servo system. The estimated performance and measured electromagnetic and structural results, as well as the preliminary observational results, are also given.

2 OPTICAL DESIGN

To design the DVA-C's optics, a set of offset Gregorian optical options with diverse parameters were set and derived, including the illumination angle and edge taper, the f/D of the main reflector, and the size of the sub-reflector. The corresponding performances of different geometries were

Table 2 Parameters of the DVA-C Optics

Aperture diameter	15 m
f/D	0.36
Sub-reflector eccentricity	0.33
Sub-reflector size	~ 5 m
Half illumination angle	55.0°
Clear distance	0.5 m
Sub-reflector tilt angle	35.2°
Tilt angle between sub-reflector and main reflector	48.1°

also simulated. Then comparisons and tradeoffs were made to best satisfy the specifications.

Figure 2 and Table 2 show the final optical design of DVA-C. The aperture of DVA-C is 15 m, with a main reflector having an 18 m maximum chord.

Considerations used in selecting DVA-C optics are listed below:

(1) Because the SKA dish will be equipped with five Single Pixel Feeds (SPFs), or three Phased Array Feeds (PAFs), a large feed illumination angle (55°) is selected to reduce the size and weights of feed assemblies. This is also suitable for most ultra-wideband feeds.
(2) An f/D ratio of 0.36 for the main reflector is selected to balance the space for feed indexer and structure deformation.
(3) A sub-reflector with a maximum chord of 5 m is chosen, to improve the aperture efficiency at lower frequency and integrate multi-beam performance with PAFs, while not significantly increasing the difficulty of fabrication.
(4) A feed-up configuration is adopted to reduce the noise due to spillover, the height of the mount and the weight of the dish structure.
(5) The reflectors are shaped to achieve the required aperture efficiency. Reflector shaping is an effective way to realize beam control, such as aperture efficiency improvement and spillover reduction. Figure 3 and Table 3 provide a comparison between the radiation pattern for shaped and unshaped optics at 1.4 GHz, assuming the DVA-C is illuminated by a Gaussian beam with –12 dB edge taper. The solid lines stand for the radiation pattern after shaping at elevation plane (Phi= 0°) and azimuth plane (Phi=90°), and the dashed lines represent the pattern before shaping. It can be seen that the gain is improved by 0.4 dB and the first sidelobe level is lower than –23 dB.

Table 3 Performance Comparison between Unshaped and Shaped Optics

Parameters	Unshaped	Shaped
Gain (dB)	45.5	45.9
3 dB beam width (°)	1.1	0.96
Aperture efficiency (%)	73.4	80.5
First sidelobe level (dB)	–28.8	–23.8

3 DISH STRUCTURE

The main reflector of DVA-C is a feed-up Gregorian dish with a turning head. Its height is 20 m and the diameter of the main reflector is 18 m×15 m while that of the sub-reflector is 5 m×4.6 m, as shown in Figure 4.

3.1 Elevation Assembly

As depicted in Figure 5, the DVA-C elevation assembly consists of a sub-reflector, main reflector and backup structure. The reflectors are made of carbon fiber reinforced polymer (CFRP), and the backup structure is composed of steel trusses.

The CFRP is an emerging material in structure unit manufacturing, with the characteristics of high stiffness-mass ratio and low thermal expansion coefficient. For these merits, CFRP is introduced in dish production, such as reflector panels, backup structures and even electrical components to improve the performance (de Lorenz et al. 2010). Combining the existing technique and novel design, the DVA-C reflectors adopt a single-piece CFRP panel with skin-and-ribs structure. The panel skin of its main reflector is an integrated and formed carbon fiber layer with 2 mm thickness, coated with aluminum spray to form a conductive surface. The backup ribs of the composite foam sandwich structure are adopted to enhance the reflector's stiffness. As shown in Figure 6, there are seven ribs along the short axis and five along the long axis.

Figure 7 illustrates the flow chart of the CFRP reflector fabrication. First, the skin and backup ribs were manufactured separately by the Vacuum Injection Molding Process (VIMP). In this way, the carbon fiber and resin were polymerized together on the mold, and solidified at a certain temperature. Then all parts were joined together by adhesive. Finally, the completed reflector was retrieved from the mold. Figure 8 displays a photo of the VIMP when the main reflector skin was being manufactured.

The sub-reflector adopts the same structure and same fabrication technology as those of main reflector, with three backup ribs in both the vertical and horizontal direc-

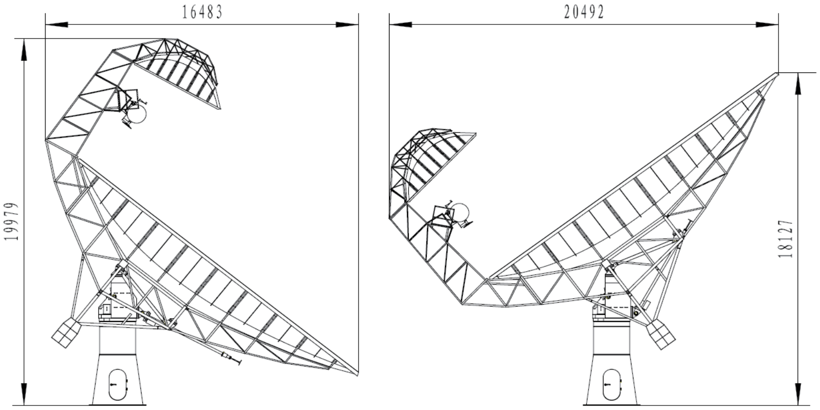

Fig. 4 Sketch Diagram of DVA-C.

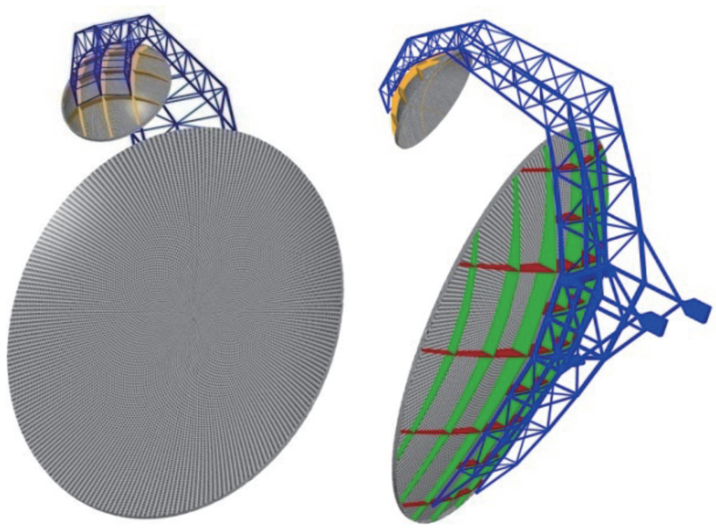

Fig. 5 Drawing of DVA-C Elevation Assemblies.

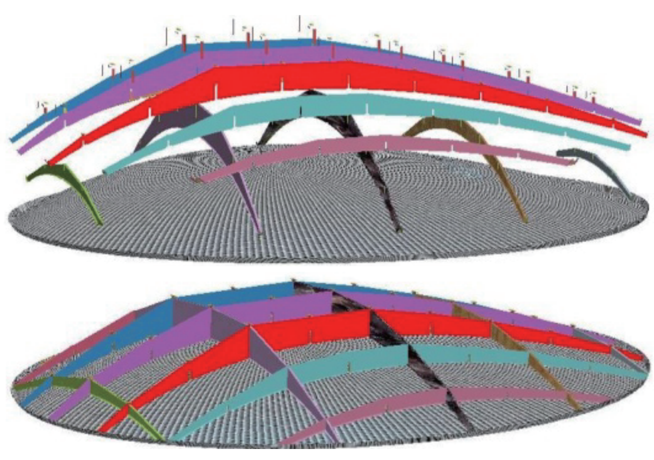

Fig. 6 Main Reflector Structure Diagram.

tions. Figure 9 depicts the finished main and sub-reflector of DVA-C.

3.2 Mount

The DVA-C adopts an altazimuth type mount, with a gear drive in azimuth and a screw drive in elevation. The mount consists of the pedestal, the azimuth part and the elevation

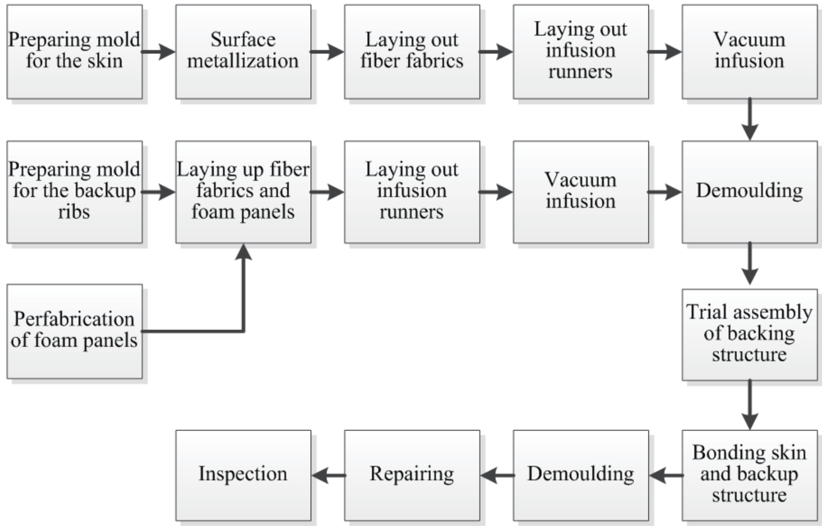

Fig. 7 Flow Chart of CFRP Reflector Fabrication.

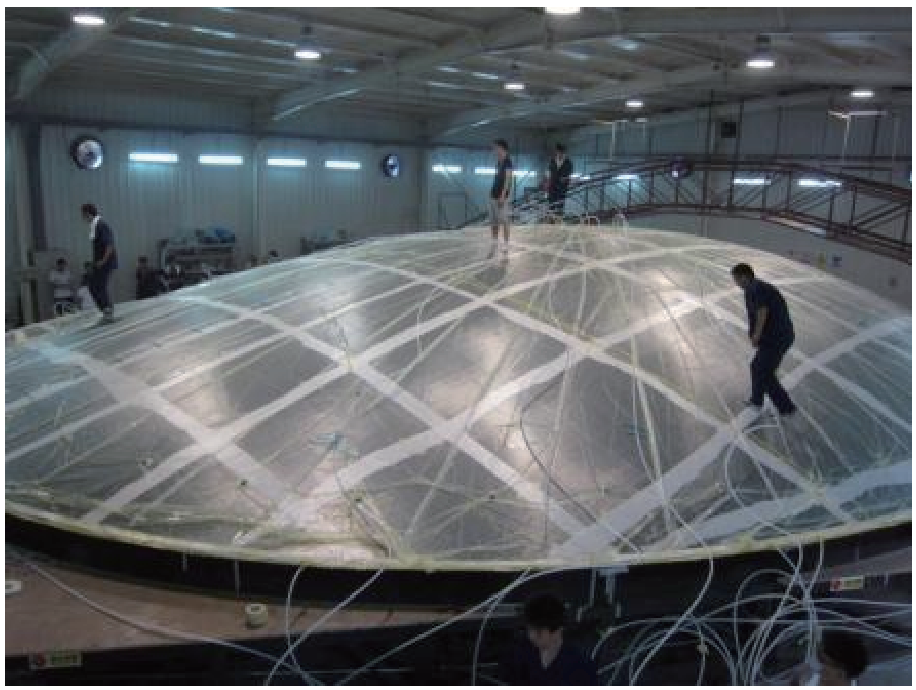

Fig. 8 Main reflector skin fabrications during the VIMP.

part, as shown in Figure 10. Considering the required mass production and maintenance, a modular design is implemented.

4 SERVO SYSTEM

The servo system consists of an antenna control unit (ACU), antenna drivers and motors, power switch and AC/DC power supplier, encoders, local control pendant, limit and safety sensors, indexer control unit (ICU), etc. The ACU, drivers ICU and AC/DC power supplier are installed inside a radio frequency interference (RFI)-tight cabinet. Figure 11 illustrates a block diagram of the antenna control system.

The main advantages of the control system are: (1) State-of-the-art components; (2) Fully digital control system; (3) Reliable real time operating system (VxWorks); (4) High reliability and safety; (5) Modular design, which is easy for maintenance; (6) RFI tightened cabinet to maintain a radio frequency (RF) quiet environment.

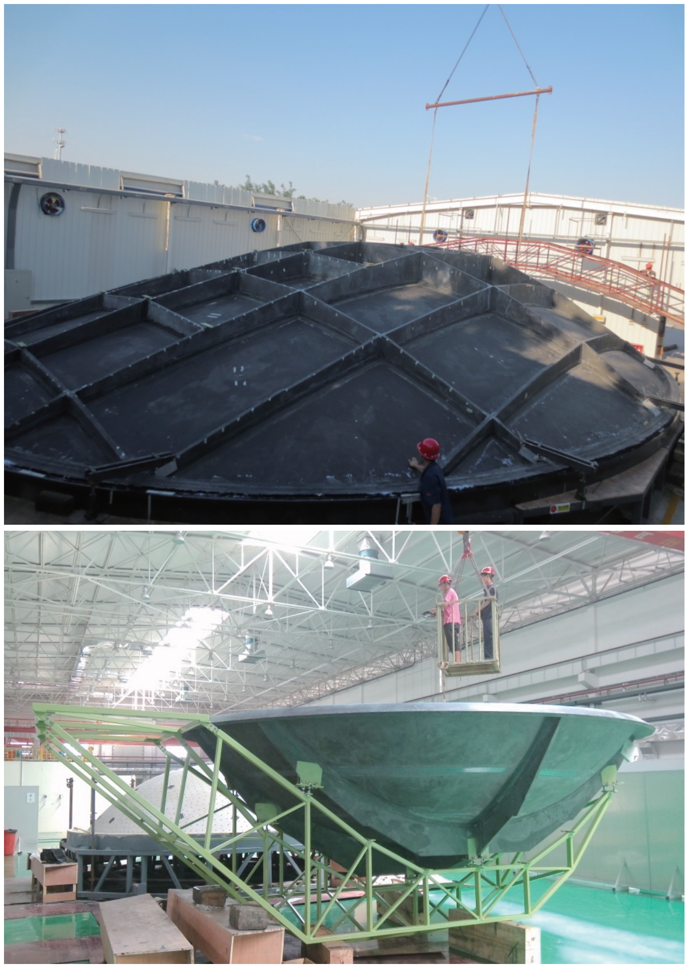

Fig. 9 Photographs of DVA-C main reflector and sub-reflector.

Fig. 10 Photograph of the DVA-C Mount.

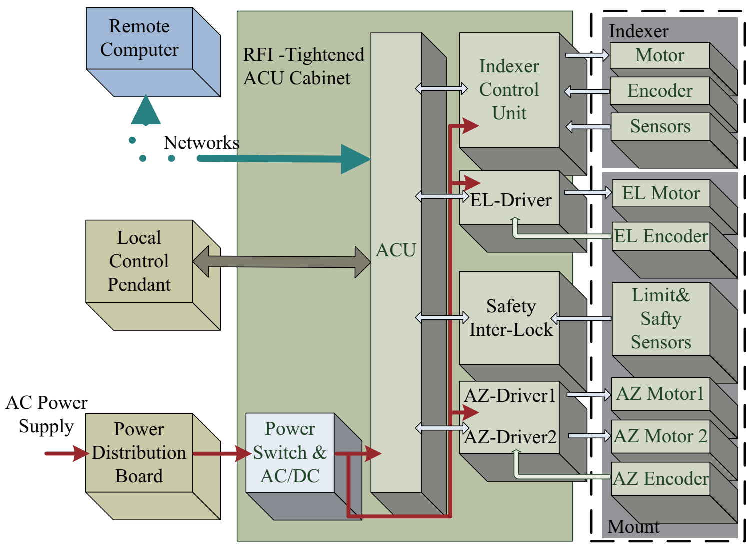

Fig. 11 Block diagram of the DVA-C control system.

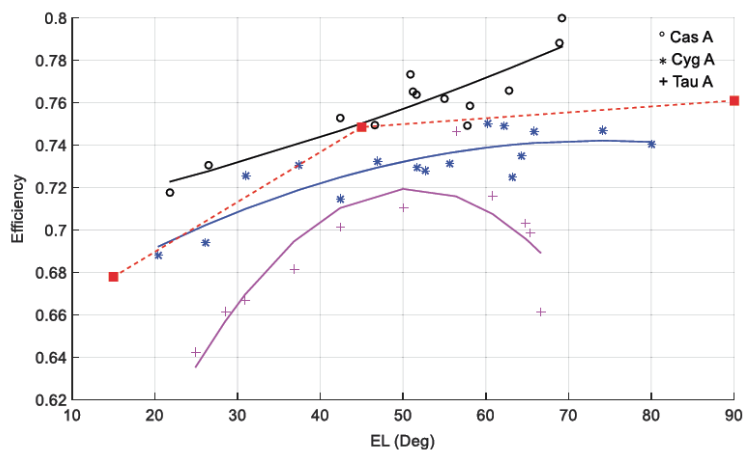

Fig. 12 Measured aperture efficiency at L band. This figure is adopted from Chai et al. (2016).

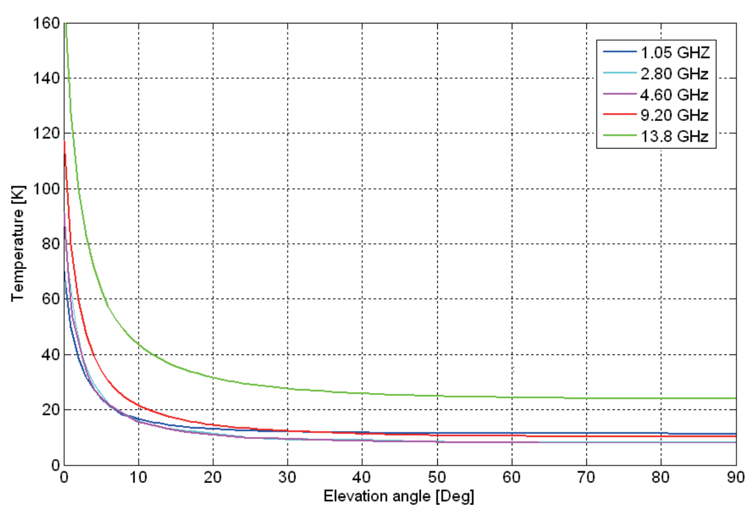

Fig. 13 Estimated environmental noise.

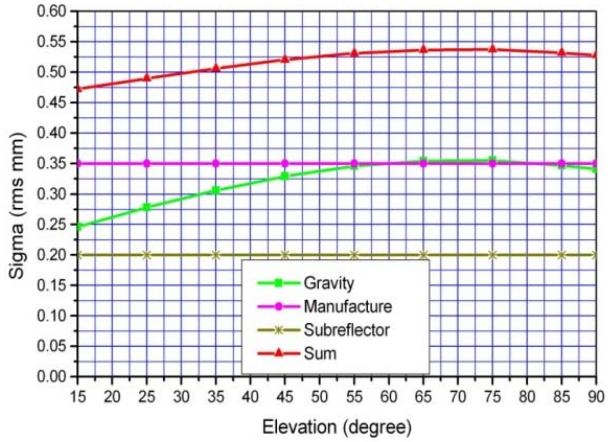

Fig. 14 Estimated DVA-C surface accuracy.

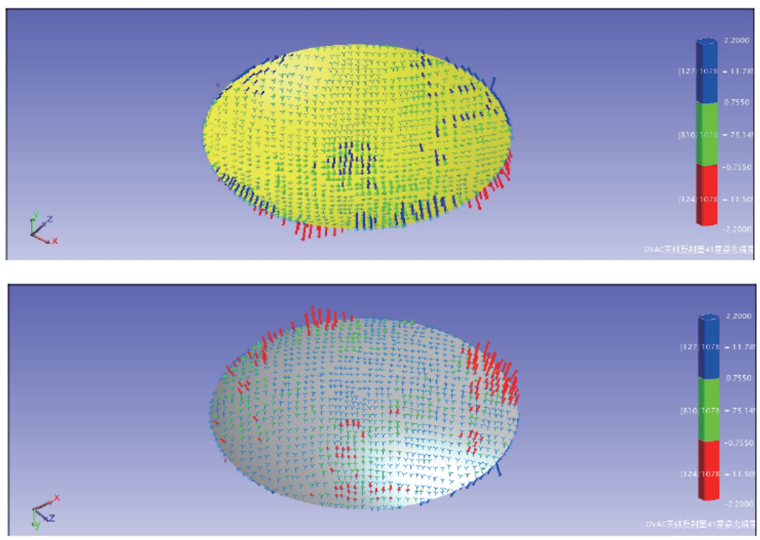

Fig. 15 Measured surface accuracy of the DVA-C @El60.

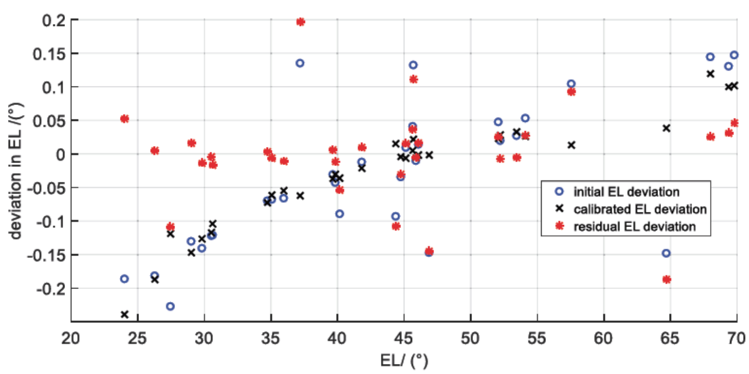

Fig. 16 Measured pointing error of the DVA-C.

5 PERFORMANCE

5.1 RF Performance

The performance of DVA-C over the operating band is estimated by GRASP[1] and given in Table 4, using a method combined with physical optics and the physical theory of diffraction. In simulation, the sub-reflector is illuminated by a Gaussian beam, with the edge taper from practical feeds. Furthermore, the surface error is assumed to be

[1] TICRA. GRASP10, Version 10.0.0 [Online]. Available: `http://www.ticra.com`.

Table 4 Estimated Performance of the DVA-C

Band	Freq (GHz)	Edge taper (dB)	First sidelobe level (dB) Estimated	Required	Aperture efficiency Estimated	Required
1	0.30	–11	–20.87		69.95	∼60
	0.35	–13	–22.63		74.30	∼65
	0.60	–16	–25.17		77.14	∼78
	1.05	–20	–29.25		74.73	∼78
2	0.95	–13.5	–24.64		79.22	∼78
	1.76	–17	–27.78		78.67	∼78
3	1.65	–13.5	–25.18	≤ -21	80.61	∼78
	3.05	–16.5	–28.82		79.22	∼78
4	2.80	–13.5	–25.53		81.41	∼78
	5.18	–16.5	–28.64		79.47	∼78
5	4.60	–13	–25.27		81.99	∼78
	9.20	–16	–28.03		78.05	∼70
	13.80	–20	–34.04		69.21	∼70

Table 5 Measured Noise Temperature of the DVA-C

Parameter	Value			Note
Fo (GHz)	3.8	7.5	12.5	Freq. in test
Y (dB)	4.3	1.97	1.7	Y factor
Tlna (K)	40	65	75	LNA noise temperature
La (dB)	0.8+0.2	1.45+0.3	1.58+0.4	Losses of cable and transducer
Tlna (K)	121.5	233.7	277.2	Tlna with La
To (K)	275	275	275	Environment temperature
Tan (K)	25.8	89.5	96.1	Antenna temperature
Lf (dB)	0.25	1.5	1.64	Loss of the feed
Ta (K)	10.8	12.8	13.8	Noise received from sky, atmosphere and ground

Table 6 DVAC Surface Accuracy Measurement Results

Element Surface Accuracy [mm]	rms
Main reflector mold:	0.352
Main reflector@ 90° El	0.707
Main reflector@ 45° El	0.755
Main reflector@ 15° El	0.795
Sub-reflector mold (modified) :	0.093
Sub-reflector (second prototype):	0.158

0.55 mm (in terms of root mean square, rms) in the efficiency calculation.

The aperture efficiency is measured by the Y factor method with three radio sources, and the results are shown in Figure 12, which is adopted from Chai et al. (2016). The red square symbols and dashed line represent the simulated result from structural Finite Element Analysis (FEA) and GRASP simulation. The other symbols and lines indicate the test results. It is worth noting that the effect of parallax is clearly seen when observing Tau A due to the intrinsic polarization of the source. The results indicate that the antenna efficiency of DVA-C is above 70% for most values of elevation.

Figure 13 shows the estimated environmental noise temperatures that are received by DVA-C at different elevation angles and different frequencies.

Table 5 gives the measured noise temperatures at different frequencies, which coincide with the simulated results.

5.2 Surface Accuracy

The reflector surface error is a key parameter in dish design, mainly depending on reflector panel manufacturing, structural alignment, gravity and environmental effects (Levy 1996). Among these effects, the errors caused by panel manufacturing, assembly and gravity stay constant

Table 7 Pointing Error Budget

Error source (rms)	Error (arcsec)	Residual error (arcsec)	Modification Method
Azimuth axis in vertical direction	10	3	Pointing model
Azimuth-Elevation non-orthogonality	15	3	-
Azimuth bearing run-out	4	4	-
Adjustment error of sub-reflector and feed	3	3	-
Gravity deformation	11	2	Lookup table
Thermal deformation	< 1	< 1	
Wind deformation	3	3	
Servo error	5	5	
Random error	3	3	
Total error (rms)		9.5 (Precision)	

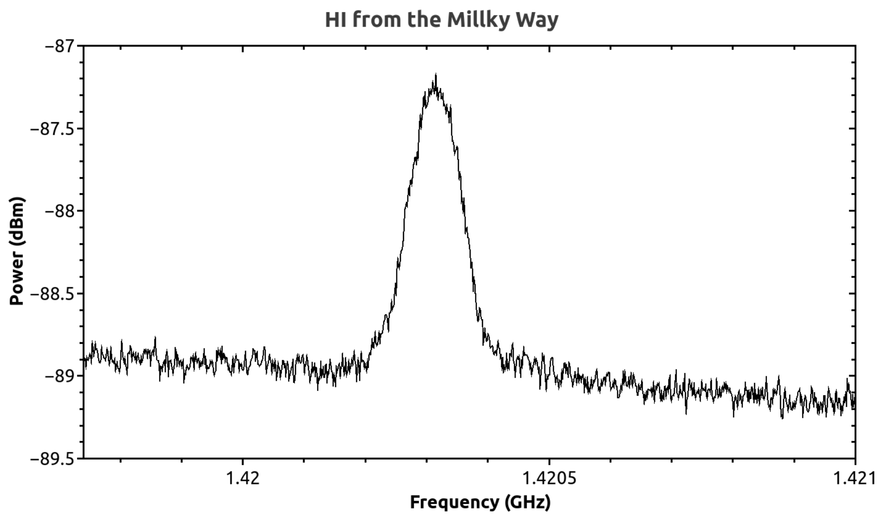

Fig. 17 The observations of neutral hydrogen in our Galaxy.

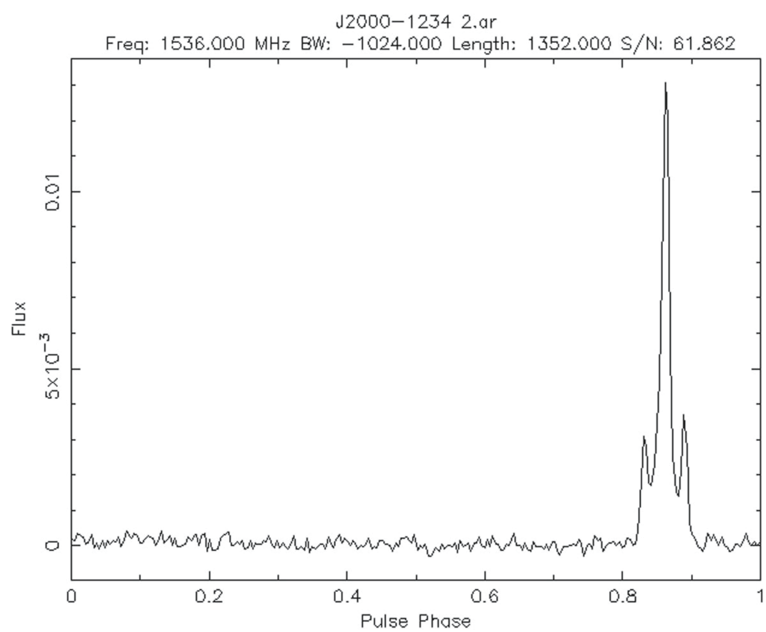

Fig. 18 The observation of pulsar B0329+54.

with time, whereas the errors from temperature and wind are random but smaller.

The structural deformation and resulting surface error of DVA-C are estimated by NASTRAN (Song et al. 2009) under gravity. Figure 14 shows the estimated surface accuracy variance with elevation angle.

Table 6 provides the measured surface accuracy of the main reflector at different elevation angles, using photogrammetry, and the measured surface accuracy results at $60°$ in elevation are illustrated in Figure 15.

5.3 Pointing Error

The antenna pointing error mostly comes from structure alignment and environment, resulting in deformation, error in servo components and movements of structural parts, such as random vibrations in gears and bearings. Among these effects, the errors from structure alignment and reflector gravitational deformation are constant and can be mostly corrected, whereas other errors are random and difficult to calibrate real time, such as temperature, wind and imperfections in components. For the errors from servo components and the moving structural parts, their effects can be alleviated by element selection and by fine fabrication. However, the errors caused by temperature and wind load can only be estimated and compensated by structure design.

The DVA-C pointing error budget is listed in Table 7, satisfying the $10''$ requirement in precision operation (at night and windless).

Pointing calibration was carried out at L band and the measured pointing error of the DVA-C at $60°$ in elevation is shown in Figure 16. The total pointing accuracy of DVA-C is about $4.7''$, which is less than one-tenth of the half power beam width (HPBW) at L band.

6 EXPERIMENTAL OBSERVATION

Since December 2014, when the first light of DVA-C was acquired, several astronomical observations targeting neutral hydrogen and pulsars have been made. For instance, Figure 17 shows observed signals from neutral hydrogen in the Milky Way and Figure 18 displays that from the pulsar B0329+54.

During the observations, DVA-C was equipped with a room temperature linear-polarization receiver centered at 1425.16 MHz. The radio frequency signal was converted down to intermediate frequency (IF) with a local oscillator frequency at 1520 MHz. The system noise temperature of DVA-C was about 110 K, including sky noise (cosmic microwave background, atmospheric loss, etc.), ground radiation from spillover, ohmic losses of the antenna, feed, wave-guide and polarizer, and receiver noise (Chai et al. 2016).

Figure 17 plots some observations of neutral hydrogen, which were made from 2016 October 09–15 with sky coverage of $10° \times 10°$ centered at longitude $49.1405°$ and latitude $-0.6028°$. During the observation, the sky area was divided into 16 $2.5° \times 2.5°$ grids, with sampling interval of $0.5°$ in each grid. So, there are 25 observations in each grid. The integration time for each observation in one grid is 2 minutes. The HI observations clearly demonstrate that the profiles shift with Galactic longitude.

Pulsar B0329+54 is one of the brightest pulsars at L band in the northern sky. It has a period of 0.714519699726 s. Figure 18 depicts an observation of this pulsar, which was made on 2016 July 14. In this observation, the IF signal was recorded by the Reconfigurable Open Architecture Computing Hardware (ROACH) backend system. ROACH performs the analog-to-digital conversion, polyphase filterbank, Fourier transform and accumulation operation to obtain the power spectrum of pulsars. An 8-bit quantization was used in both the initial digitization of the signal and the channelized output. The effective observing bandwidth in our observation is about 71.25 MHz which is divided into 228 channels. The sampling time is set to 99.2 s. The standard RFI excision, dispersion removal and pulse folding with the PSRSOFT tools were applied to data reduction of the pulsar. The integration time is 20 minutes and bandwidth is 50 MHz. From the figure, we can clearly see the profile of the pulsar as a function of observation frequency and pulse phase. Further observations will allow us to study the plasma in its magnetosphere and characteristics of the magnetic field associated with this pulsar.

Further adjustment will be carried out to improve the alignment of the DVA-C, and better results are expected.

7 CONCLUSIONS

The DVA-C is a creative dish prototype developed for the SKA, aiming at achieving high sensitivity, low cost and fast installation. Several advanced concepts are introduced in the design, especially the CFRP single-piece reflectors. After several years of effort, installation and adjustment of the DVA-C telescope have been completed, and radio signals from neutral hydrogen in the Milky Way and a pulsar have been received. These preliminary results demonstrated that DVA-C behaves reasonably well as expected, validating the design, manufacture and installation. The development of the DVA-C makes a great contribution to the SKA project. The experience gained in the DVA-C development is valuable and leads the dish scheme for the final SKA dish prototype, which is called SKA-Prototype (SKA-P). Now DVA-C has become a sample telescope for the study of radio astronomy, and it is also employed for satellite navigation research.

Acknowledgements This work is supported by the Chinese Ministry of Science and Technology under Projects of International Cooperation and Exchange (11261140641), the State Key Development Program for Basic Research (2013CB837900), the State Program for High-Tech Research and Development (SS2014AA122001) and the National Natural Science Foundation of China (Grant No. 11673031).

References

Akgiray, A., Weinerb, S., Imbriale, W. A. 2013, in 7th European Conference on Antennas and Propagation (EuCAP), Gothenburg, 768

Chai, X., Liu, B., Yu, L., et al. 2016, Experimental Astronomy, 42, 301

Davidson, D. B. 2012, in 10th International Symposium on Antennas, Propagation EM Theory (ISAPE), Xi'an, 1279

Dewdney, P. E., Hall, P. J., Schilizzi, R. T., & Lazio, T. J. L. W. 2009, IEEE Proceedings, 97, 1482

Dewdney, P. E. 2013, SKA1 System Baseline Design. Square Kilometre Array Organization, *https://www.skatelescope.org/wp-content/uploads/2013/03/SKA-TEL-SKO-DD-001-1_BaselineDesign1.pdf*

de Lera Acedo, E., Ghods, N. R., Scott, P., et al. 2012, in The 6th European Conference on Antennas and Propagation (EuCAP), Prague, 616

de Lorenz, S., Marchiori, G., Rampini, F. 2010, in Proceedings of the Fourth European Conference on Antennas and Propagation, Barcelona, 1

Hampson, G., Macleod, A., Beresford, R., et al. 2012, in International Conference on Electromagnetics in Advanced Applications (ICEAA), Jonesburg, 807

Hovey, G., Lacy, G. Byrnes, P., et al. 2014, in 16th International Symposium on Antenna Technology and Applied Electromagnetics, Victoria, 1

Imbriale, W. A., Cortes-Medellin, G., Baker, L. 2011, in IEEE Conference on Aerospace, 1

Levy, R. 1996, Structural Engineering of Microwave Antennas for Electrical, Mechanical, and Civil Engineers

Peng, B., Jin, C., Du, B., et al. 2012, Scientia Sinica Physica, Mechanica & Astronomica, 42, 1292

Song, L., Duan, B., Zheng, F., et al. 2009, Acta Electronica Sinica, 37, 553

van Ardenne, A., Bregman, J. D., van Cappellen, W. A., Kant, G. W., & de Vaate, J. G. B. 2009, IEEE Proceedings, 97, 1531

Yang, J. 2014, in XXXIth URSI General Assembly and Scientific Symposium, Beijing, 1